Stoichiometric incorporation of base substitutions at specific sites in supercoiled DNA and supercoiled recombination intermediates

Mihaela Matovina[1], Nicole Seah[2], Theron Hamilton[3], David Warren[2] and Arthur Landy[2],*

[1]Division of Molecular Medicine, Laboratory of Molecular Virology and Bacteriology, Rudjer Boskovic Institute, Zagreb, Croatia, [2]Division of Biology and Medicine, Molecular Biology, Cell Biology and Biochemistry, Brown University, Providence, RI 02912 and [3]U.S. Navy Drug Screening Laboratory, San Diego, CA 92134, USA

ABSTRACT

Supercoiled DNA is the relevant substrate for a large number of DNA transactions and has additionally been found to be a favorable form for delivering DNA and protein-DNA complexes to cells. We report here a facile method for stoichiometrically incorporating several different modifications at multiple, specific, and widely spaced sites in supercoiled DNA. The method is based upon generating an appropriately gapped circular DNA, starting from single-strand circular DNA from two phagemids with oppositely oriented origins of replication. The gapped circular DNA is annealed with labeled and unlabeled synthetic oligonucleotides to make a multiply nicked circle, which is covalently sealed and supercoiled. The method is efficient, robust and can be readily scaled up to produce large quantities of labeled supercoiled DNA for biochemical and structural studies. We have applied this method to generate dye-labeled supercoiled DNA with heteroduplex bubbles for a Förster resonance energy transfer (FRET) analysis of supercoiled Holliday junction intermediates in the λ integrative recombination reaction. We found that a higher-order structure revealed by FRET in the supercoiled Holliday junction intermediate is preserved in the linear recombination product. We suggest that in addition to studies on recombination complexes, these methods will be generally useful in other reactions and systems involving supercoiled DNA.

INTRODUCTION

Supercoiled DNA is the relevant substrate for a large number of DNA reactions, including replication initiation and elongation, transcription initiation and elongation, recombination, repair, nucleosome assembly and dynamics, regulation of gene expression, long-range enhancer effects, DNA compaction, localized melting and cruciform extrusion (1). It has additionally been found to be a favorable form for delivering DNA and protein–DNA complexes to cells (2). We report here a method that should greatly facilitate analysis of pathways involving DNA with this topology. It is a relatively facile method for stoichiometrically incorporating several different DNA modifications (we are using fluorescent dye labels and bubbles containing mismatched DNA pairs) at multiple specific sites in supercoiled DNA. The method is based upon generating an appropriately gapped circular DNA that is annealed with labeled and unlabeled synthetic oligonucleotides to make a multiply nicked circle. The circular DNA is covalently sealed and supercoiled, either by ligase in the presence of ethidium bromide, or by incubation with DNA gyrase. The method enables the stoichiometric placement of many different DNA modifications at widely spaced specific sites; it is efficient, robust and can readily be scaled up.

Our interest in developing this method grew out of a long-standing desire to study the mechanisms and structures responsible for bacteriophage λ integrative recombination—a reaction that requires supercoiled DNA substrate. Validation of the method, and several examples of its application, will be based upon this recombination reaction.

When the temperate bacteriophage λ infects an *Escherichia coli* cell under conditions unfavorable for bacterial growth or phage production, it initiates a lysogenic response that represses most of the viral genome and promotes insertion of its circular chromosome into the *E. coli* chromosome via an integrative recombination reaction. This occurs between DNA 'attachment' sites called *att*P and *att*B on the viral and bacterial

*To whom correspondence should be addressed. Tel: +1 401 863 2571; Email: Arthur_Landy@brown.edu

chromosomes, respectively. As a result, the integrated λ DNA is flanked by hybrid attachments sites, called *att*L and *att*R. In response to an improvement in the physiological state of the bacterial host, or a threat to the host's survival, λ phage DNA is excised from the chromosome by an excisive recombination between *att*L and *att*R that regenerates *att*P and *att*B on their respective circular chromosomes (3). Despite the X-ray crystal structures, genetics and biochemistry describing the individual proteins and their interactions with DNA, we still lack a comprehensive view of the λ site-specific recombination pathway. The situation is particularly unsatisfying for the integrative reaction, which has been difficult to study because it requires a supercoiled *att*P DNA substrate (4).

The integrative and excisive recombination reactions are carried out by the phage-encoded λ integrase protein (Int) by a mechanism that is common to a large family of tyrosine recombinases with diverse biological functions such as chromosome segregation, chromosome copy number control, gene expression, conjugative transposition, gene dissemination and viral integration and excision. The hallmark of this large family is a multistep reaction pathway in which a recombinase tetramer executes a sequential pair of isoenergetic strand exchanges at four 'core-type' Int binding sites, that first generate and then resolve a four-way DNA junction (Holliday intermediate) (5–8).

The λ reaction differs from that of other family members, such as Cre and Flp, in having four different recombination sites, an additional DNA-binding domain on Int, and a complex dependency upon accessory proteins that confers directionality and regulation. λ Int and its cousins comprise a subgroup of heterobivalent recombinases that bind and bridge two different families of DNA sequences (9–12). The small amino-terminal domain of Int (N-domain) binds with high affinity to five 'arm-type' binding sites distributed throughout the *att* sites and distant from the sites of strand exchange (the core-type sites). Int bridging between the arm and core sites is assisted by DNA bends induced by accessory proteins, the host-encoded IHF and the λ-encoded Xis, bound to specific sites located between the arm and core sites (Figure 1). The integration and excision reactions utilize two overlapping subsets of 16 protein binding sites to form the integrative and excisive complexes ('intasomes') that confer directionality and regulation on the recombination reaction (4). The reactions are further distinguished from each other by the unique requirement for supercoiling in *att*P DNA.

Although we shall focus on integrative recombination, the method described here for generating labeled supercoiled DNA is very general, and should be readily applicable to studying other questions in different systems.

MATERIALS AND METHODS

Int and IHF proteins were purified as described previously (13,14). Oligonucleotides were synthesized and polyacrylamide gel electrophoresis (PAGE) or high-performance liquid chromatography (HPLC) purified by Eurofins MWG Operon. Sequences of the oligonucleotides are listed in the Supplementary Tables S1, S2, S4 and S6 in the Supplemental Data. The donor dye, fluorescein and the acceptor dye, tetramethyl rhodamine (TAMRA), were attached to C5 of thymine via a 6C linker and incorporated during oligonucleotide synthesis as their respective phosphoramidites.

The dye labeling efficiency of the labeled oligonucleotides was determined from the CE and HPLC data provided by Eurofins MWG Operon. We also analyzed each fluorescently labeled oligonucleotide by 7M urea 20% PAGE to determine the percentage of fluorescent dye labeling and the overall purity of the oligonucleotides. Approximately 10 pmol of each oligonucleotide was loaded on the gel mixed with 2X formamide loading buffer (98% formamide; 1 mM EDTA pH 8; 0.0025% Xylene cyanol). Gels were run for 5 h at 25 V/cm, and then stained with SyBr gold nucleic acid gel stain (Invitrogen). Gels were scanned on Typhoon laser scanner (Amersham biosciences) and analyzed by Multi Gauge software (Fujifilm). Unmodified oligonucleotides were used as controls, which run slightly faster in the gel than the oligonucleotides modified with fluorescent dyes. We did not detect any unmodified oligonucleotide in these gels. The labeling efficiency, as determined by each of the methods, was >99%.

Single-strand phage were prepared by infecting cells carrying the appropriate pBluescript phagemid with the helper phage VCSM13, according to the protocol provided by Stratagene and scaling up to 1–31 volumes. Following extraction of the DNA with phenol–chloroform and precipitation with ethanol, the DNA was further purified by passage through a Promega Wizard SV Gel and polymerase chain reaction (PCR) Clean up column. The final yield of single-strand circular phage DNA was ~1–2 mg per liter of growth medium.

*Att*P phagemids

The *att*P DNA sequence from plasmid pWR1 (15) was copied by PCR using primers #1 and 2 (Supplementary Table S1), and cloned between the KpnI and SacI sites of phagemids pBluescript SK (+) and (–) (Stratagene). By incorporating the appropriate sequences into the 5′ adapter sequence of primer #1, an Nb.BbvCI site (CCTCAGC) was included at the KpnI junction of the product clones. The sequences of all of the primers (Supplementary Tables S1 and S2) and details of this and other cloning steps are provided in Supplementary Data. The phagemids pMM12 and pMM30 were derived from pBluescript SK (+) and (–), respectively.

Phagemid pMM13 was derived from pMM12 by changing the two T:A base pairs at the left end of the overlap region, at positions −2 and −1 (Figure 4), to A:T, using the QuikChange® II Site-Directed Mutagenesis Kit (Stratagene) and primers #3 and 4. Phagemid pMM32, for the production of gapped *att*P top-strand, was made by PCR by using primers #5 and 6, with pMM30 as a template, as described in the 'Results' section and Supplementary Data.
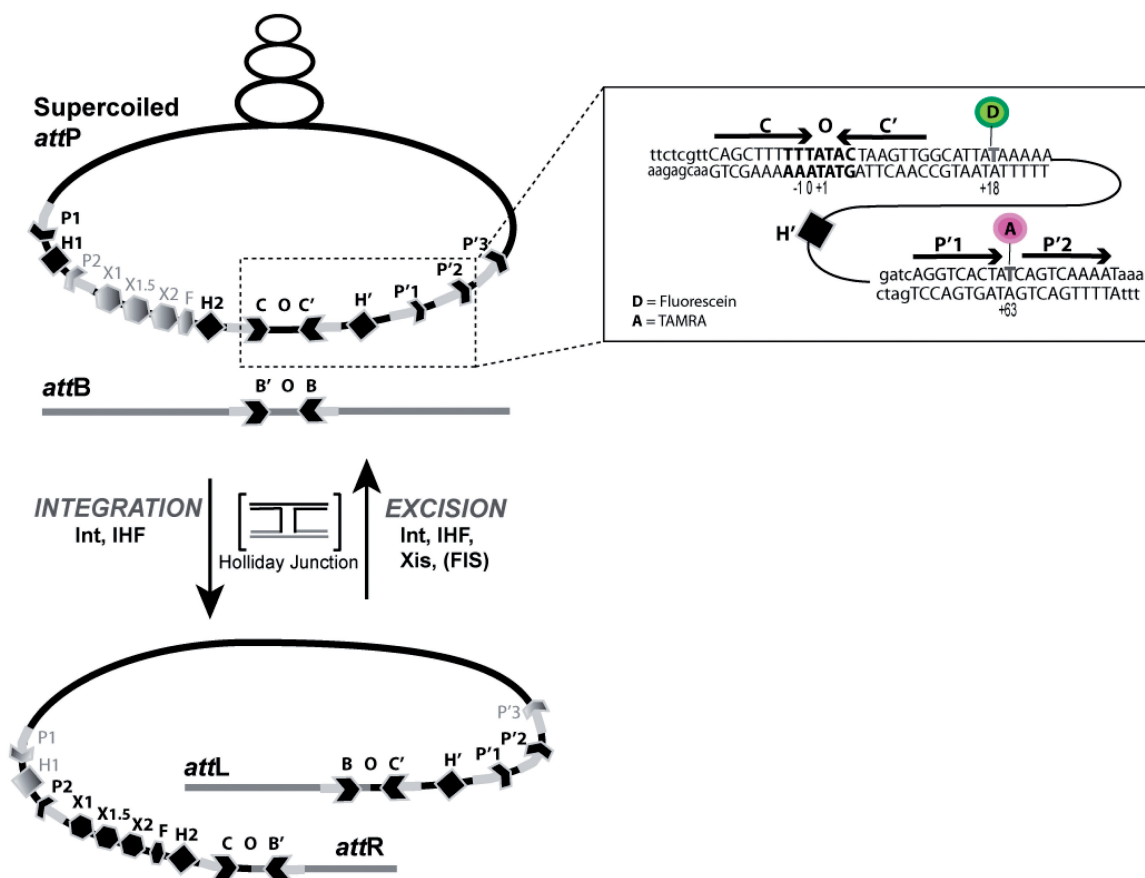
Figure 1. Schematic summary of integrative and excisive site-specific recombination. Integrative recombination between supercoiled *att*P and linear *att*B requires virally-encoded Integrase (Int) and the host-encoded accessory DNA-bending protein (IHF) and gives rise to *att*L and *att*R products. The excisive recombination between *att*L and *att*R requires the accessory DNA-bending protein Xis and is stimulated by Fis. Both reactions proceed via two pairs of sequential strand exchanges that first generate, and then resolve, a Holliday junction recombination intermediate (HJ). The four core-type Int binding sites (C, C′, B and B′; inward-facing thick arrow heads) flanking the seven bp overlap region are bound by the CB and catalytic domains of Int and form a tetrameric complex in the HJ intermediate. The arm-type Int binding sites are differentially occupied (dark thin arrow heads) by the N-domain of Int during integrative (P1, P′1, P′2 and P′3) and excisive (P2, P′1 and P′2) reactions. The IHF binding sites are differentially occupied (dark diamonds) during integrative (H1, H2 and H′) and excisive (H2 and H′) reactions. The Xis binding sites (X1, X1.5 and X2; dark hexagons) and the Fis binding site (F; dark polygon) are occupied only during the excisive reaction. (Inset) Numbering of the donor Fluorescein-labeled T (+18, D), and the acceptor, TAMRA-labeled T (+63; A) is according to previous work, where the third base pair (T) in the overlap region (bold letters) has been assigned zero and bases to its left and right are assigned negative and positive numbers, respectively (22).

*Att*B phagemids

A family tree for the mutated *att*B phagemids used to trap the Holliday junction intermediate complex is shown in Supplementary Data (Supplementary Table S3). It starts with phagemids pMM50 and pMM60, which are derived from the pBluescript SK (+) and (–), respectively. These phagemids contain *att*B inserts with a mutated overlap sequence: the TT bases at positions −2 and −1 are replaced by AA, the T at position 2 is replaced by C, and the C at position 4 is replaced by A (Figure 4). Construction of the inserts and the introduction of additional restriction sites are described in Supplementary Data. All mutagenesis steps were performed with QuikChange® II Site-Directed Mutagenesis Kit (Stratagene).

*Att*P substrate preparation

Circular single-strand (SS) DNA from phagemid pMM32 was annealed with a five-fold excess of a 45 base oligonucleotide (#17, Supplementary Table S4) complementary to the PstI–HindIII sites by heating to 80°C for 7 min in 10 mM Tris (pH 8) and 50 mM NaCl, and cooling to 4°C, in steps of 0.2°C/20 s from 80°C to 40°C, and 0.2°C/10 s from 40°C to 4°C in a gradient thermocycler (Eppendorf). This was digested with HindIII and PstI (NEB) (2 U of enzymes per 1 μg of SS DNA) at 37°C for 2 h. A mixture containing this linearized DNA, the complementary circular DNA and a 5-fold molar excess of each of the three oligonucleotides was annealed in 75 mM NaCl as described above. The nicks were sealed by incubation with T4 DNA ligase (NEB) (4 U of enzyme per 1 μg of DNA) at 16°C for 1 h. Following incubation with *E. coli* DNA Gyrase (TopoGEN, Inc.; 0.5 U of enzyme per 1 μg of total DNA) for 2 h at 37°C, the reaction was extracted three times with an equal volume of phenol/chloroform/iso-amyl alcohol (25:24:1), twice with chloroform/iso-amyl alcohol (24:1), and the covalently closed supercoiled molecules were purified by

electrophoresis overnight at 2 V/cm on 1% agarose gels. The supercoiled *att*P DNA was cut from the gel and purified with a Wizard® SV Gel and PCR Clean up system (Promega).

The heteroduplex bubble *att*P substrate was made using the same general protocol with the following DNAs: single-strand DNA from pMM13, single-strand DNA from pMM32 cleaved with PstI and HindIII, and three oligonucleotides; #18, 19 and 20 (Supplementary Table S4) for donor only substrate, or with oligonucleotides #18, 19 and 21, for donor plus acceptor substrate. *Att*P substrates for the wild-type recombination were prepared with same material, except that we used single-strand from pMM12, instead of pMM13 (Supplementary Table S5).

*Att*B substrate preparation

To prepare the long *att*B substrate for HJ trapping, circular single-strand DNA from pMM66 was annealed with the 30 base oligonucleotide (#22, Supplementary Table S6), complementary to the region around the NheI site at position 2711, and digested with NheI (2 U of enzyme per 1 μg of DNA, at 37°C for 2 h). The linearized single-strand DNA was annealed to circular single-strand DNA from pMM55, and the annealed product was linearized with HindIII to produce a nicked linear 2.9 kb *att*B. Phenol extraction, gel electrophoresis, and purification of the eluted linear *att*B were carried out as described above. The *att*B was dephosphorylated with Antarctic phosphatase (NEB) and labeled with ^{32}P at the 5′ termini using T4 polynucleotide kinase (NEB).

Short *att*B substrate for wild-type recombination was prepared by annealing top-strand oligonucleotide #23 (Supplementary Table S6), which was 5′ end-labeled with ^{32}P using T4 polynucleotide kinase (NEB), to the bottom-strand oligonucleotide #24 (Supplementary Table S6). Oligonucleotides #23 and 24 were annealed in the 1:1 ratio in 10 mM TRIS (pH 8) and 50 mM NaCl. The mixture was put in the boiling water bath, and cooled to room temperature overnight.

*Att*P by *att*B integrative recombination

Integrative recombination reactions were performed by incubating supercoiled *att*P and radioactively labeled *att*B with 60 nM Int and 60 nM IHF in 25 mM Tris, pH 8, 5 mM EDTA, pH 8, 0.5 mg/ml bovine serum albumin (BSA), 2.5 mM DTT, 75 mM NaCl and 6 mM spermidine for 1 h on 25°C. Wild-type reactions were resolved by electrophoresis in 1% agarose/0.4% Synergel (Diversified Biotech), while Holliday junction intermediate trapping reactions were resolved in a 1% agarose gel, at 5 V/cm for 3–3.5 h, respectively. Reactions designed to generate *att*L and *att*R recombinant products contained 20 nM supercoiled *att*P and 40 nM short *att*B substrate. Reactions designed to generate Holliday junction intermediates contained 20 nM supercoiled *att*P bubble substrate and 20 nM radioactively labeled *att*B bubble/heterology substrate, as described in the text.

In-gel Förster resonance energy transfer

Förster resonance energy transfer (FRET) was determined by measuring the extent of donor fluorescence quenching in a donor plus acceptor reaction relative to the fluorescence in a donor only reaction. In the former, *att*P substrates were labeled with fluorescein at position P+18, near the C′ core site, and with TAMRA at position P+63, between the P′1 and P′2 sites. In the latter, *att*P substrates were labeled only with fluorescein at position P+18 (see Figure 1).

Recombination and Holliday junction reactions (50 μl each) were prepared according to the protocols for *att*P by *att*B recombination described above and incubated at 25°C for 1 h. One-sixth volume of loading buffer was added to each reaction (15% ficoll in 6X TAE buffer) and either four (7, 9.5, 12.5 and 16 μl) or five (4, 7, 10, 13 and 16 μl) aliquots of each reaction was electrophoresed for 3–3.5 h at 5 V/cm on a 1% agarose/ 0.4% Synergel gel for wild type recombination or a 1% agarose gel for Holliday junction intermediates. The gels were scanned on a Typhoon laser scanner (Amersham Biosciences) with the blue laser (488 nm), and a 520-nm emission filter to measure the fluorescence of the fluorescein in complexes with and without TAMRA. The amount of the recombinant product or HJ complex was determined after drying the gel, exposing it on an imaging plate (Fujifilm), and scanning the imaging plate using BAS 2500 system (Fujifilm). The fluorescence intensity and the amount of ^{32}P were determined for each band using Multigauge software (Fujifilm).

FRET calculations

The efficiency of energy transfer was determined by measuring the extent of donor quenching in the HJ complexes with both donor and acceptor dyes, as previously described (16), based on following equation:

$$I_i^{DA} \frac{[\text{complex}]_j^D}{[\text{complex}]_i^{DA}} = I_j^D (1 - rE)$$

where I_j^D is the fluorescence intensity of the donor in the Holliday junction band *j*, labeled with donor (D) only; I_i^{DA} is the fluorescence intensity of the Holliday junction band *i*, labeled with both D and acceptor (A) dyes; $[\text{complex}]_j^D$ and $[\text{complex}]_i^{DA}$ are the total amounts of the Holliday junction complex labeled with D only and with A plus D, respectively, as determined from the phosphorimager scan of the gel; *r* is the efficiency of DNA labeling with acceptor; and *E* is the efficiency of energy transfer.

The fluorescence intensities of the donor plus acceptor complexes (I_i^{DA}) are corrected for the differences in the total amounts of the complex, between donor-only and donor plus acceptor complexes, using the ratio of $[\text{complex}]_j^D / [\text{complex}]_i^{DA}$, determined from the radioactivity scans. An average value for ($I_i^{DA}/[\text{complex}]_i^{DA}[\text{complex}]_j^D$) was determined as described in Supplementary Data. The standard deviation for each point in this averaging process was less than ±0.05. All of the values in the plot were normalized to 1 by dividing by the highest donor intensity of the donor-only complex

bands. The line was constructed from data collected in three or four independent experiments. In a plot of (I_i^{DA}/[complex]$_i^{DA}$[complex]$_j^D$) (*y*-axis), versus the fluorescence intensity of the donor only complex, I_j^D (*x*-axis), the slope of the line equals $1 - rE$. As described above and in the 'Results' section, we have determined that the oligonucleotides are substituted with TAMRA to >99%. As a complete complement of oligonucleotides is required to obtain supercoiled DNA (data not shown), $r = 1$ in all of the TAMRA-labeled supercoiled DNA substrates.

RESULTS

Summary of the method

Phagemids, in addition to their own plasmid origin of replication, contain a phage origin of replication, such that infection of a host cell by an appropriate helper phage leads to production of phage particles containing a circular DNA corresponding to one strand of the phagemid (17,18). The choice of which DNA strand is replicated and packaged is determined by the orientation of the viral origin of replication within the phagemid (19,20). We used pBluescript SK ± phagemids (Stratagene), which contain a 454 bp intergenic region from filamentous phage f1 (M13 related) that includes the 307-bp phage origin of replication oriented in one direction (+) or the other (–) (21). Our procedure starts by cloning the DNA region of interest in two phagemids that differ only in the orientation of their respective origins of phage DNA replication (see Figure 2A for schematic summary). One of them, phagemid A(+), is used directly to make circular single-strand phage DNA that will comprise the 'template' strand of a gapped circular DNA molecule.

DNA from the other phagemid, A(–), is used to direct a series of PCR reactions leading to a family of deletion phagemids, that will ultimately give rise to the 'non-template' strands, which will flank gaps of different sizes in the region of interest. A PCR primer that will ultimately define the right side of a gap has a 5′ adapter sequence (not complementary to the template) encoding a BamHI site followed by a PstI site and then DNA sequence complementary to the template on the right side of the gap (primer #5; Supplementary Table S1). A primer that will ultimately define the left side of a gap has a 5′ adapter sequence encoding a BamHI site followed by a HindIII site and then DNA sequence complementary to the template on the left side of the gap (primer #6; Supplementary Table S1). The linear products of PCR amplification are cut with BamHI, circularized by ligating the annealed overhangs, and used to generate the B(–) family of phagemids.

Circular single-strand DNA made from the B(–) family of phagemids is linearized by annealing it with a 45 base oligonucleotide complementary to the HindIII–PstI region and cleaving with those two enzymes. The resulting linear single-strand DNA is complementary to the circular single-strand template DNA made from Phagemid A(+), except for the DNA sequence that was deleted in the PCR reactions. Using HindIII and PstI sites enables placement of the gap boundaries between any A and any G in the region of interest. Different 5′-and 3′-overhang restriction sites can be used to obtain bases other than A or G at the gap boundaries.

The gap resulting from annealing the linear deletion strand and the full-length circular strand is filled in by annealing with the appropriate labeled and unlabeled synthetic oligonucleotides (38–51 bases long) to generate a nicked circular molecule that is then sealed by DNA ligase. Negative supercoiling can be introduced either by the presence of ethidium bromide during ligation or by incubation with DNA gyrase (Figure 2). The final supercoiled molecule will have a 454-nt bubble corresponding to the identical origins of replication.

Recombination of supercoiled *att*P labeled with fluorescein and TAMRA

We cloned a 371-bp DNA fragment containing *att*P and some flanking sequences [from pWR1 (15)] between the KpnI and SacI sites of pBluescript II SK (+) and pBluescript II SK (–), creating phagemids pMM12 and pMM30, respectively. DNA derived from pMM12 phage particles [A(+) DNA in Figure 2] was used directly for making one strand of *att*P DNA, referred to as the 'bottom' strand, in conformance with previous nomenclature for the *att* site DNAs (22). DNA derived from pMM30 phagemid [A(–) DNA in Figure 2] was used as the template for making a linear PCR product deleted for a portion of the *att*P region. In these experiments, the primer specifying the left side of the deletion had 3′-terminal sequences complementary to positions −26 to −38 of the *att*P region. The primer specifying the right side of the deletion had 3′ terminal sequences complementary to sequences immediately adjacent to the right side of the *att*P region. Both primers had 5′-terminal adapter sequences, as described above and illustrated in Figure 2A. The resulting linear PCR fragment was circularized and used to generate phagemid pMM32. This will be the source of the top strand [B(–) in Figure 2], which, when annealed to the bottom strand derived from pMM12, will produce a top-strand deletion of 136 bases (extending downstream from the H1 site in the P arm and spanning the entire P′ arm) (Figure 1).

To construct the supercoiled *att*P, the circular SS DNA from pMM32 phage was linearized by digestion with PstI and HindIII (after annealing with a complementary 45 base synthetic oligonucleotide) and annealed with the circular SS pMM12 template strand to generate a 136-base gap. The gap was filled in by annealing with a 5-fold excess of three complementary synthetic oligonucleotides, 51, 38 and 47 bases in length. Following incubation with ligase and DNA gyrase the supercoiled *att*P was purified by gel electrophoresis.

In anticipation of the FRET experiments described below, one of the synthetic oligonucleotides used to fill in the 136-base gap contained a donor dye (dT-fluorescein) at position +18 and another oligonucleotide contained an acceptor dye (dT-TAMRA) at position +63 (see 'Materials and Methods' section). The dye-labeling efficiency of the fluorescently labeled

A Methodology for preparing dye-labeled *att*P
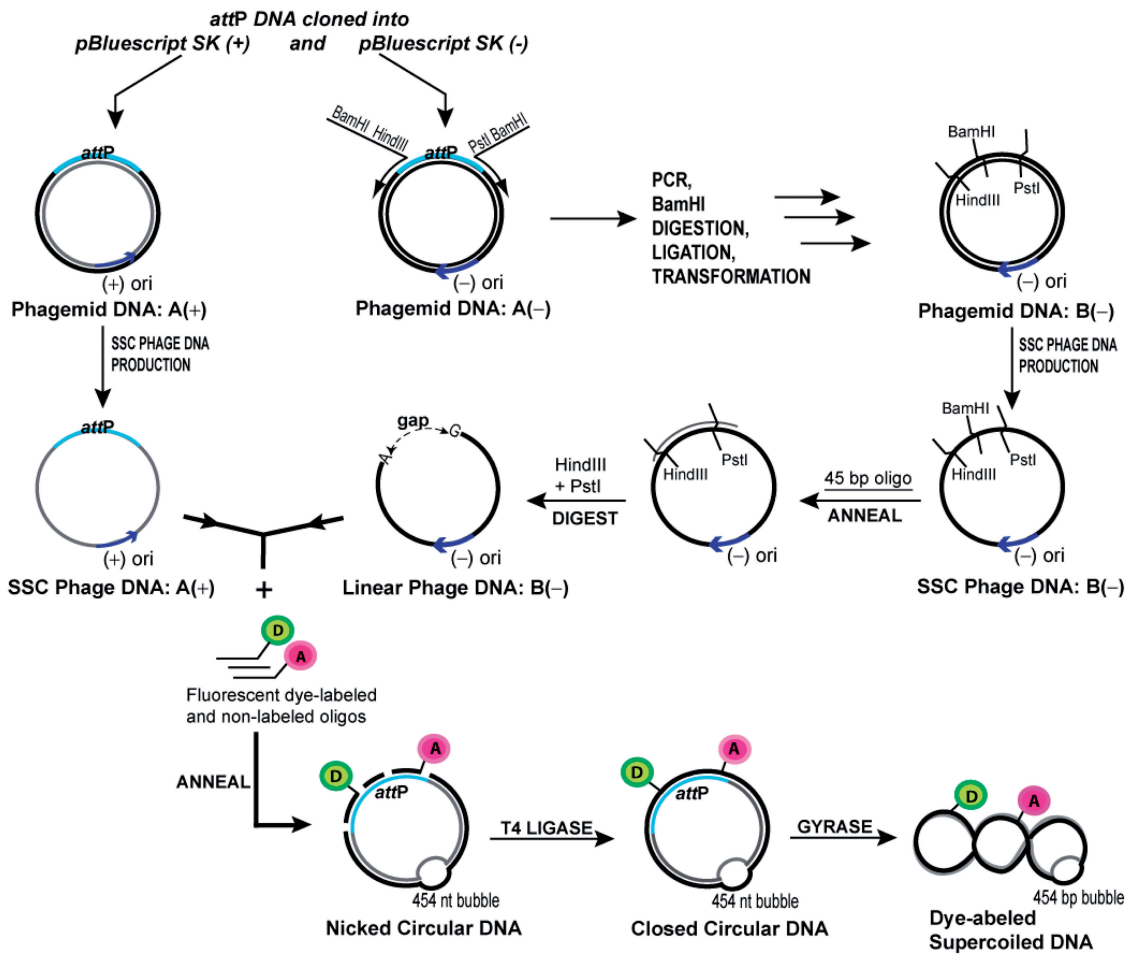
B Analysis of dye-labeled *att*P
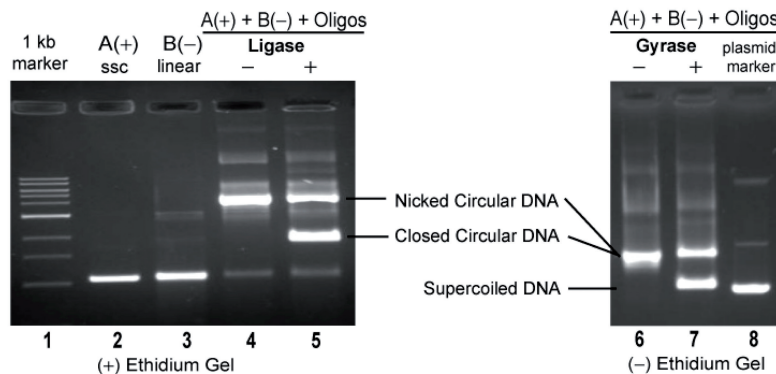
Figure 2. Preparing supercoiled DNA labeled with fluorescent dyes. (**A**) Schematic summary of the method. Single-strand circular *att*P DNA from Phagemid DNA A(–) is used as the template for a PCR reaction that will give rise to the 'non-template' strand that will define (flank) the gap over a selected portion of *att*P. The left side of the gap is defined by a primer that has a 5′ adapter sequence (not complementary to the template) encoding a BamHI site followed by a HindIII site and then DNA sequence complementary to the template on the left side of the gap. The right side of the gap is defined by a primer that has a 5′ adapter sequence encoding a BamHI site followed by a PstI site and then DNA sequence complementary to the template on the right side of the gap. The linear products of PCR amplification are cut with BamHI, circularized by ligating the annealed overhangs, and used to generate the B(–) family of phagemids. Circular single-strand DNA made from the B(–) family of phagemids [SSC Phage DNA B(-)] is linearized by annealing it with a 45-base oligonucleotide complementary to the HindIII–PstI region and cleaving with those two enzymes. The resulting linear single-strand DNA, which corresponds to the 'top-strand' of *att*P, is annealed to the single-strand circular DNA made from phagemid A(+), which corresponds to the 'bottom-strand' of *att*P [SSC Phage DNA A(+)]. Included in the annealing mixture are oligonucleotides that will fill in the designed gap and will bring in the specified acceptor (A) and/or donor (D) fluorescent dyes. The resulting nicked circle is incubated with ligase to generate covalently closed circular DNA that is then supercoiled by incubation with DNA gyrase to generate the final dye-labeled DNA. (**B**) Electrophoresis of the DNA intermediates and products in a 1% agarose gel with (lanes 1–5), or without (lanes 6–8), ethidium bromide

oligonucleotides was determined to be >98–99% as determined by three different methods: capillary electrophoresis and HPLC data provided by the manufacturer (Eurofins MWG Operon); and by the ratio of labeled to unlabeled oligonucleotides separated by gel electrophoresis in 20% polyacrylamide, 7 M urea. The labeling efficiency of acceptor dye-labeled oligonucleotides was also checked by determining the ratio of the absorbances of the dye and the oligonucleotide, which also showed that dT-TAMRA labeling efficiency is >98–99% (see 'Materials and Methods' section).

The yield of covalently closed circular *att*P is ~60% (Figure 2B, lane 5). We have also made molecules in which the top strand deletion comprises the entire *att*P region: when this 263 base gap is filled in by annealing with 5 nt the yield of closed circular *att*P is approximately 40% (data not shown). The conversion of covalently closed circles to supercoiled molecules by incubation with *E. coli* DNA gyrase is very efficient (Figure 2B, lane 7), while the final yield of the supercoiled molecules, from preparative scale agarose gels, is ~15–20%. At the scale of these experiments, we routinely recover at least 10 μg of labeled supercoiled *att*P DNA. Purification and recovery of large quantities of the supercoiled product by CsCl$_2$ density gradient centrifugation should be much more efficient than gel electrophoresis, making this method very easy to scale up. The supercoiled dye-labeled *att*P was tested for recombination with a ^{32}P-labeled 60-bp oligonucleotide encoding the *att*B partner, and was found to be comparable to supercoiled plasmid DNA in kinetics (data not shown) and dependence upon Int concentration (Figure 3).

Trapping supercoiled Holliday junction recombination intermediates

The Holliday recombination intermediate is formed by a DNA strand swap on the left side of a seven base pair 'overlap' region that must be identical between the recombination partners. It is resolved to fully duplex recombination products by a DNA strand swap on the right side of the overlap region (5,23–25). Thus, in the 7-bp overlap region of the recombination products, each DNA strand originates from a different partner (Figure 4). A sequence difference between the overlap regions of two partners blocks recombination (24). On the other hand, partners carrying unpaired bubbles within their overlap region will recombine as long as the swapped strands recreate a paired duplex in the recombinant products (26). Reversal of this top-strand exchange would result in reformation of the unpaired bases and is thus not favored. We have combined these two observations to efficiently trap Holliday recombination intermediates (Figure 4) [see also ref (27)]. The appropriate unpaired bubbles on

the left side of the *att*P and *att*B overlap region promote, and prevent reversal of, the first (top) strand swap. A sequence difference between the partners on the right side of the overlap region prevents execution of the second (bottom) strand swap and thus prevents resolution of the Holliday junction (23,28).

To generate the phagemid for producing the bottom strand of a heteroduplex bubble *att*P, we changed the two T:A base pairs at the left boundary of the overlap region in pMM12, at positions −2 and −1, to A:T base pairs, to create pMM13. Phage particles from pMM13 yield the bottom strand of *att*P with an overlap sequence of 3′-TTATATG-5′ (instead of the wild-type sequence 3′-AAATATG-5′). The heteroduplex bubble in *att*P is generated during the annealing with top-strand synthetic oligonucleotides, because the oligonucleotide complementary to the overlap region has the wild-type top-strand sequence, 5′-TTTATAC-3′. Additionally, some of the top-strand synthetic oligonucleotides contained a dT-fluorescein and/or a dT-TAMRA fluorescent dye at positions +18 and +63, respectively, as described above (Figure 1).

Preliminary experiments indicated that during agarose gel electrophoresis good separation of a Holliday junction intermediate from other reaction components required a long *att*B partner. We therefore cloned the 42 bp of *att*B sequence and flanking DNA between the KpnI and SacI sites of a pair of pBluescript II SK (+) and (–) phagemid vectors to generate pMM50 and pMM60, respectively. We introduced additional restriction sites for NheI and HindIII in those two vectors, leading to the creation of pMM55 and pMM66 phagemids (see 'Materials and Methods' section, and Supplementary Data). Annealing the single strands from pMM66 and pMM55 generates the AA left-side 2-bp bubble in *att*B (complementary to the TT bubble generated in *att*P). Additionally, the sequence on the right side of the *att*B overlap region, while perfectly paired, differs from the *att*P overlap at positions 2 and 4 (Figure 4).

To make the *att*B recombination partner, we linearized circular SS DNA from pMM66 by digesting with NheI (after annealing a 30-base oligo complementary to the target NheI site at position 2711 of the AttB plasmid sequence). This linear DNA was then annealed with circular SS DNA from pMM55 and the resulting nicked circle was linearized by digestion with HindIII and purified by agarose gel electrophoresis.

Recombination between the supercoiled *att*P and linear *att*B partners described above does not yield the linear recombination product seen with wild-type substrates. Rather, we observe a new product with properties of the anticipated supercoiled Holliday junction intermediate. The fluorescent dye from the *att*P partner and the

(0.5 μg/ml). Following electrophoresis the DNA was visualized by staining with ethidium bromide. A 1-kb ladder (NEB) (lane 1) and a supercoiled plasmid DNA (lane 8) serve as markers. Lane 2, single-strand circular phage DNA [A(+) SSC], encoding the bottom strand of *att*P (from pMM12); lane 3, linearized phage DNA [B(–) linear], encoding truncated top-strand sequences of *att*P (from pMM32); lane 4, the nicked circle resulting from annealing the linearized B(–) DNA and the circular A(+) DNA, along with the gap-filling oligonucleotides; lane 5, the mixture of covalently closed and nicked circles after incubation with ligase; lane 6, the DNA from lane 5 electrophoresed in the absence of ethidium bromide; lane 7, the mixture of supercoiled and nicked DNA following incubation with DNA gyrase.
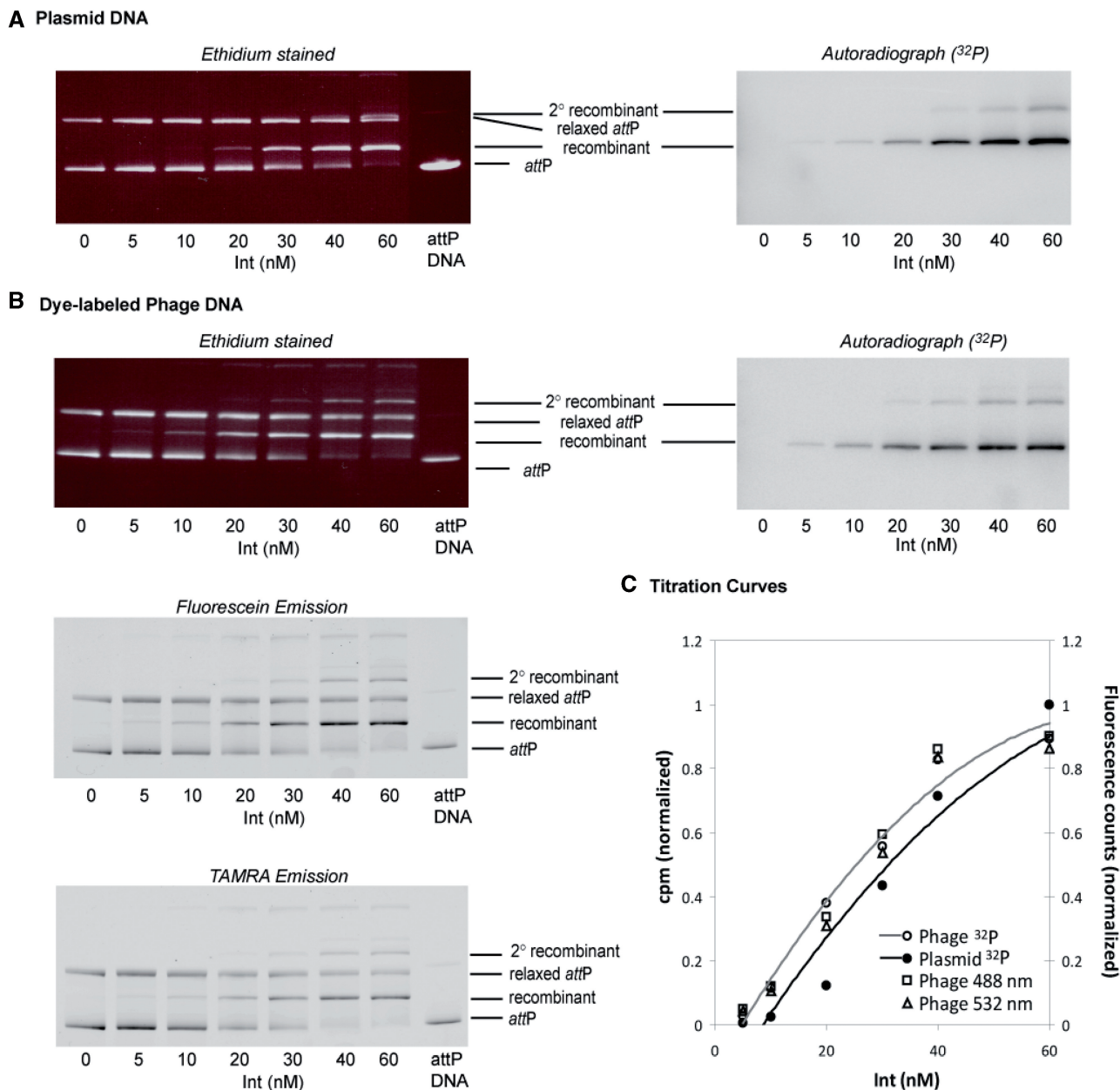
Figure 3. Comparison of recombination efficiencies of supercoiled *att*P as plasmid or dye-labeled phage DNA. Recombination reactions between a 60-bp ^{32}P-radiolabeled *att*B (run off the gel) and supercoiled *att*P, either as plasmid DNA (**A**) or as fluorescein- and TAMRA-labeled phage DNA (**B**) were carried out with the indicated concentrations of Int at 25°C for 1 h and then resolved by gel electrophoresis (1% agarose and 0.4% Synergel), as described in 'Materials and Methods' section. (**C**) Gels containing the dye-labeled phage DNA were scanned for fluorescence by fluorescein (excited at 488 nm) and by TAMRA (excited at 532 nm) (lower left panels); then all of the gels were stained with ethidium bromide (top left panels). The ^{32}P label from *att*B was visualized by autoradiography and the fluorescence intensity and the amount of ^{32}P were quantified using Multigauge software, as described in 'Materials and Methods' section, and in the text.

^{32}P label from the *att*B partner are both present in the new product (Figure 5, lane 3). When the new product is recovered from the native agarose gel, deproteinized and re-electrophoresed, no linear recombination product is observed, and if it is digested with the restriction enzyme KpnI, it does not generate the fragments expected from a linear recombination product (data not shown). If a 60-bp *att*B is used in place of the large *att*B, the ^{32}P label from the *att*B that was incorporated into the new product has the same mobility as supercoiled *att*P, as would be expected for a supercoiled Holliday junction with two very short linear arms (data not shown). Finally, when the putative Holliday junction product is digested with the nicking enzyme Nb.BbvCI (which has a single target in the *att*P DNA), the mobility is reduced, as expected for the conversion from a supercoiled to a relaxed circular molecule (Figure 5, lane 4). We conclude that the substrates designed to trap supercoiled Holliday junction intermediates of integrative recombination are working as predicted.
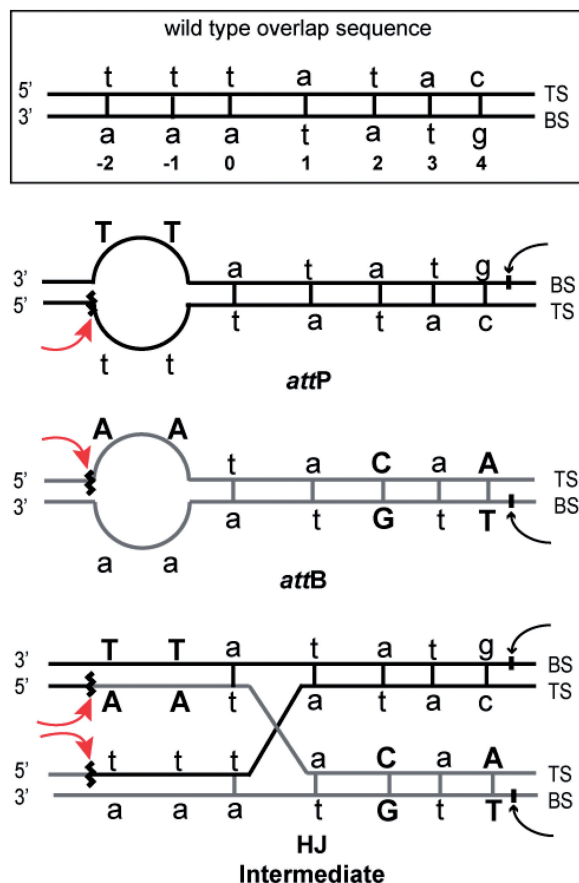
Figure 4. Overlap regions of the *att*P and *att*B sites showing the bubble–heterology sequences used to trap Holliday junction recombination intermediates. The altered base pairs of the 7-bp overlap region are indicated in bold upper case letters, the Int cleavage sites flanking each overlap region are indicated by curved arrows, and the strands conventionally referred to as the top- and bottom-strands are labeled TS and BS, respectively; numbering is the same as in Figure 1. To highlight the salient features of these sites, three modifications to the conventional depictions have been made: (a) the two *att* sites are aligned in a parallel rather than antiparallel orientation; (b) the *att*P site is drawn with the 'top strand' (TS) on the bottom; and (c) as a result of the parallel alignment of the *att* sites, the exchanged strands in the Holliday junction (HJ) are crossed. Following the first pair of Int cleavages the top strands are swapped to form the Holliday junction, simultaneously converting the unpaired (bubble) bases to the more stable duplex DNA. The second pair of Int cleavages on the bottom strands that would normally resolve the Holliday junction to recombinant products (attL and attR) is strongly disfavored because the sequence differences between the two overlap regions would generate unpaired bubbles in both *att*L and *att*R after strand exchange. The resulting Holliday intermediate is thus stabilized with respect to both the reverse and forward reaction products.

Comparison of FRET measurements on the supercoiled Holliday junction intermediate and a linear recombination product

Current views of the λ site-specific recombination pathway predict the collaboration of accessory DNA bending proteins and the bivalent DNA binding of λ integrase to bring some of the distal arm-type sites into close proximity with the core-type Int binding sites (where strand exchange takes place) (4). However, we have only limited notions of which higher-order structures form, change, or dissolve during the course of a recombination reaction. The ability to position multiple DNA modifications at different loci within supercoiled DNA opens the door on several experimental approaches to addressing these questions for the integrative pathway. In the following experiments, we have used FRET to probe and compare an element of higher-order structure in the supercoiled integrative Holliday junction and the linear recombination product.

In the absence of any higher-order structure, the linear distance in base pairs between the fluorescein donor dye at position +18 (adjacent to the C′ core-type site) and the acceptor TAMRA dye at position +63 (between the P′1 and P′2 arm-type sites) greatly exceeds the maximum distance (~100 Å) over which energy can be transferred by FRET. The long linear *att*B partner for trapping Holliday junctions was constructed and labeled with ^{32}P at the 5′ termini, as described above and in 'Materials and Methods' section. In addition to this 'donor plus acceptor' reaction, a parallel 'donor only' reaction was carried out under the same conditions with a heteroduplex bubble *att*P containing only the fluorescein donor dye at position +18.

Following incubation with Int and IHF, different amounts of each reaction were loaded in adjacent lanes and fractionated by native agarose gel electrophoresis. The gels were scanned in a Typhoon laser scanner with the Blue laser (488 nm) and a 520-nm emission filter. The amount of Holliday junction complex in each lane was quantified from a Phosphor-Imager scan of the ^{32}P-labeled *att*B. The efficiency of energy transfer (E) was determined from the extent of quenching of the donor fluorescence (520 nm) in the complexes labeled with donor plus acceptor compared with the complexes labeled with donor only. The comparison was facilitated by using the same ^{32}P-labeled *att*B to form both sets of Holliday junction complexes, thus enabling normalization of the fluorescence of each band to the amount of complex in that band.

A typical gel scanned for donor fluorescence (left panel) and radioactivity (right panel) is shown in Figure 6A. The quantified data from four experiments was combined to generate the plot in Figure 6C, left panel, as described in 'Materials and Methods' section. From the slope of the line, which equals $1 - E$, the average FRET efficiency from these four experiments is 23%.

We then asked whether the higher-order structure reflected by this FRET in the supercoiled Holliday junction complex was lost or retained during the progression to a linear recombinant product. We constructed a supercoiled *att*P substrate without the heteroduplex bubble but labeled with the donor and acceptor dyes in the same positions as the above experiment. This was recombined with a duplex linear *att*B that had the same overlap region sequence as the *att*P partner, thus leading to a complete *att*L plus *att*R linear recombinant product. These reactions were fractionated by native agarose gel electrophoresis (Figure 6B) and the average FRET efficiency in the recombinant product, determined from three experiments,
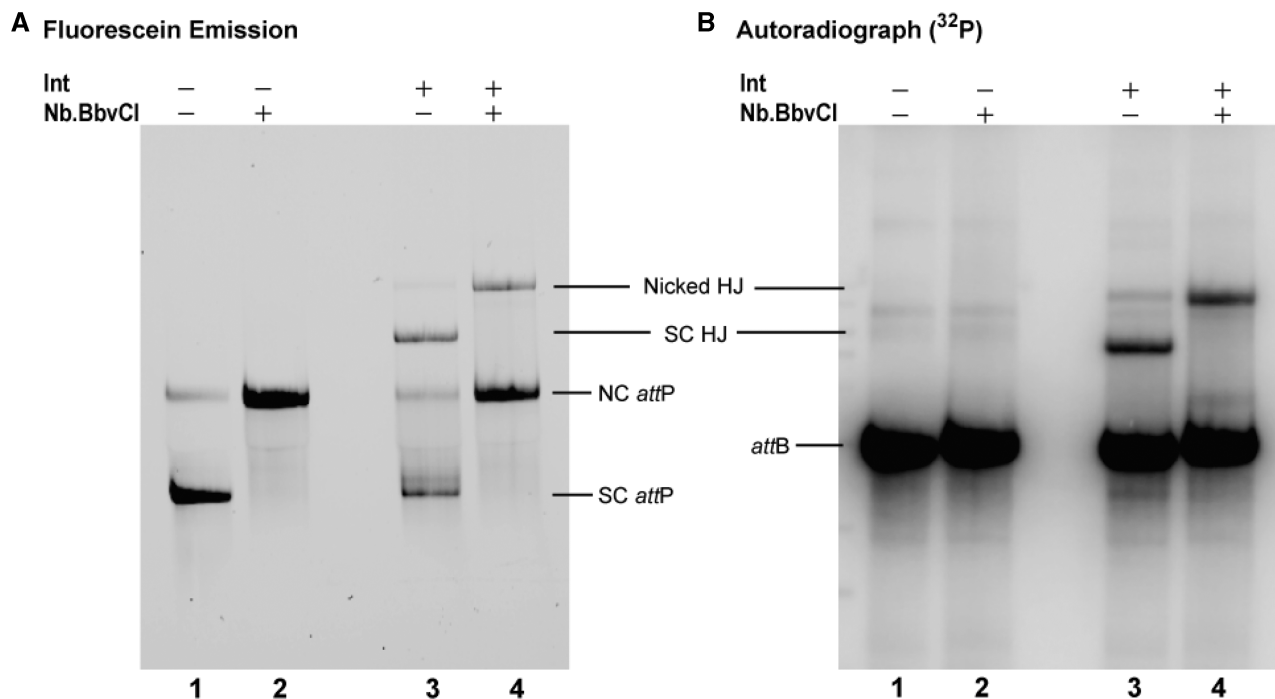
Figure 5. Trapping a dye-labeled supercoiled Holliday junction recombination intermediate and its relaxation by site-specific nicking with the restriction enzyme Nb.BbvCI. Recombination reactions with the HJ-trapping *att* sites diagramed in Figure 4 were carried out with dye-labeled supercoiled *att*P and linear ^{32}P-labeled *att*B, and analyzed by agarose gel electrophoresis, as described in 'Materials and Methods' section. (**A**) Visualization of the gel by 488-nm excitation of fluorescein in *att*P. (**B**) Visualization of the gel by autoradiography of the ^{32}P-radiolabel in *att*B. Recombination reactions, without (lanes 1 and 2), or with (lanes 3 and 4), Int were incubated for 1 h, after which MgCl$_2$ (10 mM final) and the nicking enzyme, Nb.BbvCI were added to reactions 2 and 4, and all four reactions were incubated for an additional hour before loading onto a native agarose gel. No full recombination product is formed under these conditions. In control reactions with canonical *att* sites, the nicking enzyme does not alter the mobility of the full linear recombination product (data not shown).

as described above, was found to be 18% (Figure 6C, right panel).

The close similarity between the FRET efficiencies of the two dye pairs, identically positioned in the supercoiled Holliday junction and the linear recombinant product strongly suggests that the portion of the higher-order structure identified by this FRET is preserved in both complexes.

DISCUSSION

The majority of previous approaches to incorporating labels into covalently closed circular DNA can be grouped into two categories. The first group is based on the initial approach of Zoller and Smith (29) using a short synthetic oligonucleotide, complementary to the circular single-strand DNA, as a primer for DNA polymerase. A number of modifications and enhancements, such as using different polymerases, the addition of different ensembles of accessory proteins, and different reaction conditions, have been devised to reduce the limitations of low yields and/or displacement of the labeled oligonucleotide primer by polymerase elongating around the circle (30,31). The second group consists of various methods for constructing gapped molecules, which were then filled in with a single oligonucleotide. Circular ssDNA was used as the source of one strand and an appropriate duplex DNA (made either

by restriction endonuclease digestion or by PCR) as a source of the second strand (32).

The method we have described here for incorporating a large number of synthetic oligonucleotides, any or all of which can carry a variety of different labels and/or DNA modifications, is well suited for analyses involving FRET. It is likely to be advantageous in many other types of analyses, as well. In the experiments reported here, we used three oligonucleotides to fill in a gap of 136 bp but we have also made supercoiled *att*P substrates using five oligonucleotides to fill in a 263-bp gap with acceptable overall yields. In those cases where there are no constraints on the DNA sequences at one or both boundaries of the gap, the method can be simplified by using only one restriction enzyme to cut the ssDNA.

One of the features of the gapped molecule approach that is essential for our studies is the assurance that substrates are homogeneous and completely labeled. Our method is also well suited for experiments in which multiple labels must be positioned and/or repositioned throughout the course of a study. This method can be readily scaled up to produce large quantities of labeled supercoiled DNA for biochemical and structural studies, in which case it might be advantageous to replace the final gel electrophoresis purification of supercoiled substrate with CsCl$_2$ density gradient centrifugation.

The FRET experiments reported here indicate the feasibility of this approach to studying the integrative
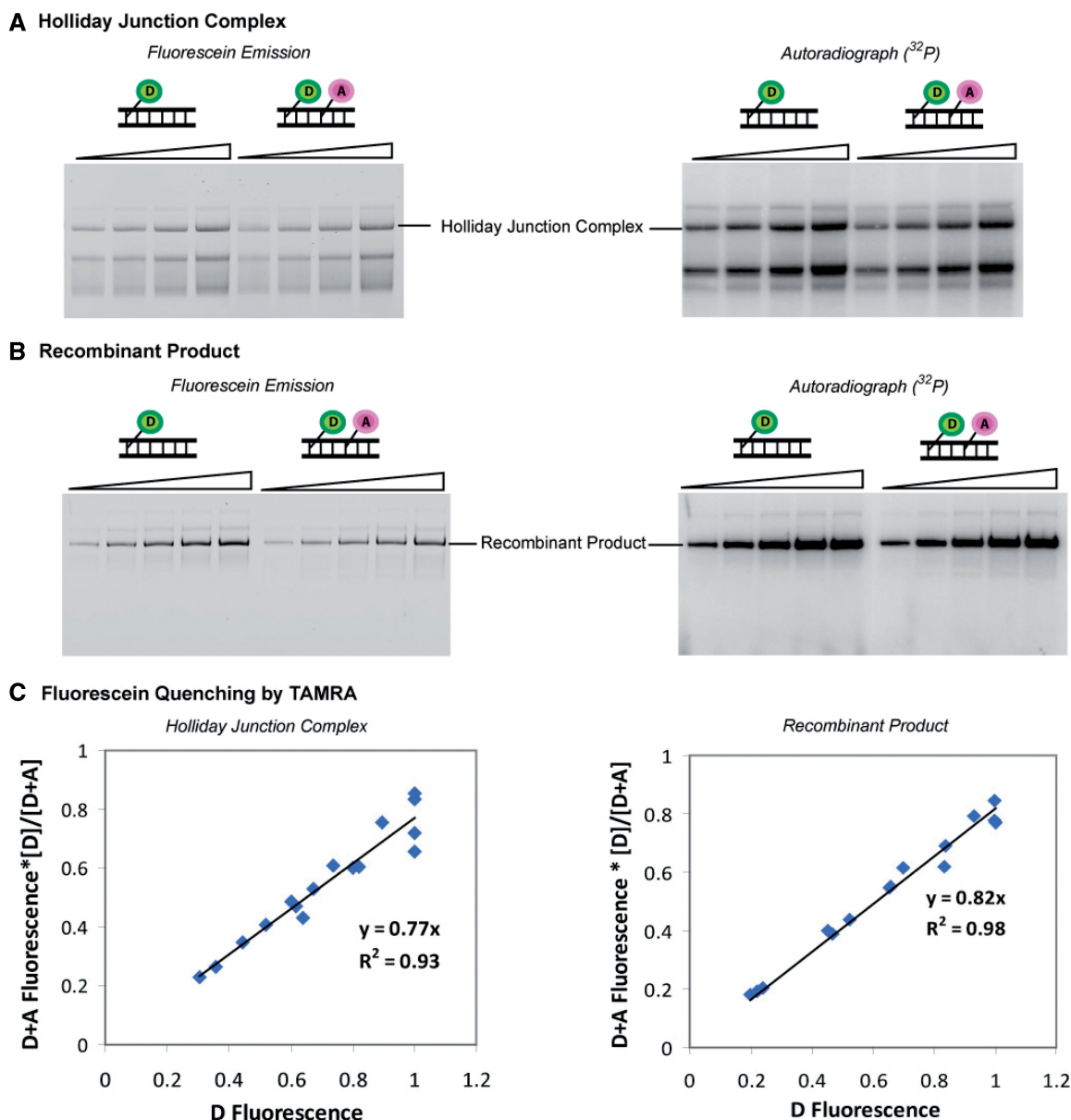
Figure 6. Comparison of FRET within the Holliday junction complex and the recombination product. Integrative recombination reactions between a pair of bubble/heterology *att* sites, to yield Holliday junction complexes (**A**), or a pair of canonical *att* sites, to yield full recombinant product (**B**), were carried out, and the resulting protein–DNA complexes were analyzed by agarose gel electrophoresis, as described in 'Materials and Methods' section. The supercoiled *att*P DNAs were labeled with fluorescein donor dye (D) at position +18, plus or minus TAMRA acceptor dye (A) at position +63 (see inset of Figure 1). A*tt*B was radiolabeled with ^{32}P at its 5′ termini. Different size aliquots (7, 9.5, 12.5 and 16 μl for the HJ and 4, 7, 10, 13 and 16 μl for the recombinant) were loaded onto each lane (rising wedge). (**C**) The donor fluorescence and ^{32}P radioactivity of the Holliday junction and recombinant complexes were quantified using Multigauge software as described in 'Materials and Methods' section, and in the text. The values on the *y*-axis, ($I_i^{DA}/[\text{complex}]_i^{DA}[\text{complex}]_j^{D}$), are the donor fluorescence in the donor plus acceptor complexes multiplied by the ratio of ^{32}P radioactivity in the donor only versus the donor plus acceptor complexes (averaged as described in Supplementary Data). The values for the *x*-axis are the fluorescence of the donor in the corresponding donor only complexes, I_j^{D}. The slope of the line is $1 - rE$, where E is the energy of transfer, and in our experiments $r = 1$, as described in 'Materials and Methods' section, and the text.

recombination reaction, and, by extension, many other reactions in a wide range of systems that depend upon or utilize supercoiled DNA. The specific placement of labels and DNA modifications in supercoiled substrates should be particularly helpful in studies on the initiation and elongation steps of both replication and transcription, nucleosome positioning and many pathways of recombination (33–36). Biophysical studies of DNA, including the

internal dynamics of supercoiled DNA are also likely beneficiaries of such substrates (37).

A potentially practical application of site-specifically modified supercoiled DNA is in the area of non-viral gene delivery into eukaryotic cells and non-viral gene therapy (2). Among the modifications used to improve gene delivery to the nucleus are DNA–peptide conjugates, called nuclear localization sequences (NLS) (38).

However, most of the methods used thus far do not allow controlled addition of NLS peptide molecules to supercoiled DNA (39). This could be important, since a single NLS attached to a DNA molecule is sufficient for nuclear entry, while several peptides might inhibit entry (40). Additionally, too many chemical modifications of the delivery DNA (and/or in the wrong place) could inhibit transcription (41). [For a recent review see ref. (42).]

According to the Förster theory (43), the efficiency of resonance energy transfer E is related to the distance between the donor and acceptor, R, by the equation: $E = R_0^6/(R_0^6 + R^6)$, where R_0 is the distance between the donor and acceptor that gives 50% FRET (the Förster distance). There are many factors complicating accurate determination of R_0 (44); however, in the experiments reported here, the donor and acceptor dyes are in the same immediate environment (with respect to DNA sequence and protein neighbors) such that, whatever the precise value of R_0, it should be the same in both the Holliday junction and the recombinant product. In other words, the ratio of the two FRET energies will be a measure of the ratio of the physical distances: $(R_1/R_2) = \sqrt[6]{E_2(1 - E_1)/E_1(1 - E_2)}$. The values (Figure 6 and text above) for E_1 (from the Holliday junction complex), and E_1 (from the recombinant product complex), are 0.23 and 0.18, respectively, yielding 0.95 for the approximate ratio of the distances observed in the Holliday junction and product complexes.

These data strongly indicate that the portion of the higher-order structure revealed by FRET in the supercoiled Holliday junction intermediate is preserved in the linear recombination product. This had been an open question and the results raise additional questions about how many other features of the Holliday junction intermediate are preserved in the products and which of these preserved and/or altered features contributes to the directionality and regulation of the recombination reaction. Fortunately, the experiments reported here also open the door to answering many of the questions that have been raised in regard to the integrative reaction. It is not unreasonable to expect these methods, which are efficient, robust and readily scaled up, will also be useful in other reactions and systems involving supercoiled DNA.

SUPPLEMENTARY DATA

Supplementary Data are available at NAR Online.

ACKNOWLEDGEMENTS

REFERENCES

1. Kanaar,R. and Cozzarelli,N.R. (1992) Roles of supercoiled DNA structure in DNA transactions. *Curr. Opin. Struct. Biol.*, **2**, 369–379.
2. Iqbal,K., Barg-Kues,B., Broll,S., Bode,J., Niemann,H. and Kues,W. (2009) Cytoplasmic injection of circular plasmids allows targeted expression in mammalian embryos. *BioTechniques*, **47**, 959–968.
3. Campbell,A.M. (1962) In Caspari,E.W. and Thoday,J.M. (eds), *Advances in Genetics.* Academic Press, New York, pp. 101–145.
4. Azaro,M.A. and Landy,A. (2002) In Craig,N.L., Craigie,R., Gellert,M. and Lambowitz,A. (eds), *Mobile DNA II.* ASM Press, Washington, DC, pp. 118–148.
5. Hsu,P.L. and Landy,A. (1984) Resolution of synthetic *att* -site Holliday structures by the integrase protein of bacteriophage λ. *Nature*, **311**, 721–726.
6. Kitts,P.A. and Nash,H.A. (1988) An intermediate in the phage λ site-specific recombination reaction is revealed by phosphorothioate substitution in DNA. *Nucleic Acids Res.*, **16**, 6839–6856.
7. Van Duyne,G.D. (2001) A structural view of Cre-*lox*P site-specific recombination. *Annu. Rev. Biophys. Biomol. Struct.*, **30**, 87–104.
8. Chen,Y. and Rice,P.A. (2003) New insight into site-specific recombination from Flp recombinase-DNA structures. *Annu. Rev. Biophys. Biomol. Struct.*, **32**, 135–139.
9. Nunes-Düby,S., Tirumalai,R.S., Kwon,H.J., Ellenberger,T. and Landy,A. (1998) Similarities and differences among 105 members of the Int family of site-specific recombinases. *Nucleic Acids Res.*, **26**, 391–406.
10. Rudy,C., Taylor,K.L., Hinerfeld,D., Scott,J.R. and Churchward,G. (1997) Excision of a conjugative transposon in vitro by the Int and Xis proteins of Tn 916. *Nucleic Acids Res.*, **25**, 4061–4066.
11. Hickman,A.B., Waninger,S., Scocca,J.J. and Dyda,F. (1997) Molecular organization in site-specific recombination: the catalytic domain of bacteriophage HP1 integrase at 2.7 Å resolution. *Cell*, **89**, 227–237.
12. Lewis,J.A. and Hatfull,G.F. (2003) Control of directionality in L5 integrase-mediated site-specific recombination. *J. Mol. Biol.*, **326**, 805–821.
13. Sarkar,D., Azaro,M.A., Aihara,H., Papagiannis,C., Tirumalai,R.S., Nunes-Düby,S.E., Johnson,R.C., Ellenberger,T. and Landy,A. (2002) Differential affinity and cooperativity functions of the amino-terminal 70 residues of λ integrase. *J. Mol. Biol.*, **324**, 775–789.
14. Hazelbaker,D., Azaro,M.A. and Landy,A. (2008) A biotin interference assay highlights two different asymmetric interaction profiles for lambda integrase arm-type binding sites in integrative versus excisive recombination. *J. Biol. Chem.*, **283**, 12402–12414.
15. Hsu,P.L., Ross,W. and Landy,A. (1980) The λ phage *att* site: functional limits and interaction with Int protein. *Nature*, **285**, 85–91.
16. Radman-Livaja,M., Biswas,T., Mierke,D. and Landy,A. (2005) Architecture of recombination intermediates visualized by In-gel FRET of λ integrase-Holliday junction-arm-DNA complexes. *Proc. Natl Acad. Sci. USA*, **102**, 3913–3920.
17. Cleary,J.M. and Ray,D.S. (1980) Replication of the plasmid pBR322 under the control of a cloned replication origin from the single-stranded DNA phage M13. *Proc. Natl Acad. Sci. USA*, **77**, 4638–4642.
18. Dotto,G.P., Enea,V. and Zinder,N.D. (1981) Functional analysis of bacteriophage f1 intergenic region. *Virology*, **114**, 463–473.

19. Messing,J. and Vieira,J. (1982) A new pair of M13 vectors for selecting either DNA strand of double-digest restriction fragments. *Gene*, **19**, 269–276.

20. Dente,L., Cesareni,G. and Cortese,R. (1983) pEMBL: a new family of single stranded plasmids. *Nucleic Acids Res.*, **11**, 1645–1655.

21. Short,J.M., Fernandez,J.M., Sorge,J.A. and Huse,W.D. (1988) Lambda ZAP: a bacteriophage lambda expression vector with in vivo excision properties. *Nucleic Acids Res.*, **16**, 7583–7600.

22. Landy,A. and Ross,W. (1977) Viral integration and excision: structure of the lambda *att* sites. *Science*, **197**, 1147–1160.

23. Nunes-Düby,S., Matsumoto,L. and Landy,A. (1987) Site-specific recombination intermediates trapped with suicide substrates. *Cell*, **50**, 779–788.

24. Weisberg,R.A., Enquist,L.W., Foeller,C. and Landy,A. (1983) Role for DNA homology in site-specific recombination: the isolation and characterization of a site affinity mutant of coliphage lambda. *J. Mol. Biol.*, **170**, 319–342.

25. Kitts,P.A. and Nash,H.A. (1988) Bacteriophage λ site-specific recombination proceeds with a defined order of strand-exchanges. *J. Mol. Biol.*, **204**, 95–107.

26. Bauer,C.E., Hesse,S.D., Gardner,J.F. and Gumport,R.I. (1984) DNA interactions during bacteriophage lambda site-specific recombination. *Cold Spring Harbor Symp. Quant. Biol.*, **49**, 699–705.

27. Sun,K.Q. (1990) A study of DNA-DNA interactions during bacteriophage lambda integrative recombination. Doctoral Thesis in Biochemistry. University of Illinois at Urbana-Champaign.

28. Burgin,A.B. and Nash,H.A. (1995) Suicide substrates reveal properties of the homology-dependent steps during integrative recombination of bacteriophage λ. *Curr. Biol.*, **5**, 1312–1321.

29. Zoller,M.J. and Smith,M. (1982) Oligonucleotide-directed mutagenesis using M13-derived vectors: an efficient and general procedure for the production of point mutations in any fragment of DNA. *Nucleic Acids Res.*, **10**, 6487–6500.

30. Kodadek,T. and Gamper,H. (1988) Efficient synthesis of a supercoiled M13 DNA molecule containing a site specifically placed psoralen adduct and its use as a substrate for DNA replication. *Biochem.*, **27**, 3210–3215.

31. Bregeon,D. and Doetsch,P.W. (2004) Reliable method for generating double-stranded DNA vectors containing site-specific base modifications. *BioTechniques*, **37**, 760–766.

32. Pine,R. and Huang,P.C. (1987) An improved method to obtain a large numer of mutants in a defined region of DNA. *Methods Enzymol.*, **154**, 415–430.

33. Leng,F., Amado,L. and McMacken,R. (2004) Coupling DNA supercoiling to transcription in defined protein systems. *J. Biol. Chem.*, **279**, 47564–47571.

34. Fullwood,M.J., Liu,M.H., Pan,Y.F., Liu,J., Xu,H., Mohamed,Y.B., Orlov,Y.L., Velkov,S., Ho,A., Mei,P.H. *et al.* (2009) An estrogen-receptor-[agr]-bound human chromatin interactome. *Nature*, **462**, 58–64.

35. Nakagawa,T., Bulger,M., Muramatsu,M. and Ito,T. (2001) Multistep chromatin assembly on supercoiled plasmid DNA by nucleosome assembly protein-1 and ATP-utilizing chromatin assembly and remodeling factor. *J. Biol. Chem.*, **276**, 27384–27391.

36. Forte,P., Leoni,L., Sampaolese,B. and Savino,M. (1989) Cooperativity in nucleosomes assembly on supercoiled pBR322 DNA. *Nucleic Acids Res.*, **17**, 8683–8694.

37. Kalkbrenner,T., Arnold,A. and Tans,S.J. (2009) Internal dynamics of supercoiled DNA molecules. *Biophys. J.*, **96**, 4951–4955.

38. Martin,M.E. and Rice,K.G. (2007) Peptide-guided gene delivery. *AAPS J.*, **9**, E18–E29.

39. Escriou,V., Carrière,M., Scherman,D. and Wils,P. (2003) NLS bioconjugates for targeting therapeutic genes to the nucleus. *Adv. Drug Delivery Rev.*, **55**, 295–306.

40. Zanta,M.A., Belguise-Valladier,P. and Behr,J.P. (1999) Gene delivery: a single nuclear localization signal peptide is sufficient to carry DNA to the cell nucleus. *Proc. Natl Acad. Sci. USA*, **96**, 91–96.

41. Nagasaki,T., Myohoji,T., Tachibana,T., Futaki,S. and Tamagaki,S. (2003) Can nuclear localization signals enhance nuclear localization of plasmid DNA? *Bioconjug. Chem.*, **14**, 282–286.

42. Lam,A.P. and Dean,D.A. (2010) Progress and prospects: nuclear import of nonviral vectors. *Gene Ther.*, **17**, 439–447.

43. Förster,T. (1948) Intermolecular energy migration and fluorescence. *Ann. Phys.*, **2**, 55–75.

44. Ivanov,V., Li,M. and Mizuuchi,K. (2009) Impact of emission anisotropy on fluorescence spectroscopy and FRET distance measurements. *Biophys. J.*, **97**, 922–929.